Thinking small: next-generation sensor networks close the size gap in vertebrate biologging

Simon P. Ripperger[1,2,3,*], Gerald G. Carter[2,3], Rachel A. Page[2], Niklas Duda[4], Alexander Koelpin[5], Robert Weigel[4], Markus Hartmann[6], Thorsten Nowak[6], Jörn Thielecke[6], Michael Schadhauser[6], Jörg Robert[6], Sebastian Herbst[7], Klaus Meyer-Wegener[7], Peter Wägemann[8], Wolfgang Schröder-Preikschat[8], Björn Cassens[9], Rüdiger Kapitza[9], Falko Dressler[10], Frieder Mayer[1,11]

[1]Museum für Naturkunde, Invalidenstraße 43, 10115 Berlin, Germany

[2]Smithsonian Tropical Research Institute, Apartado 0843-03092, Balboa, Ancón, Republic of Panama

[3]Department of Evolution, Ecology, and Organismal Biology, The Ohio State University, Columbus, OH, USA

[4]Institute for Electronics Engineering, Friedrich-Alexander University Erlangen-Nürnberg (FAU), Wetterkreuz 15, 91058 Erlangen-Tennenlohe, Germany

[5]Chair for Electronics and Sensor Systems, Brandenburg University of Technology, Siemens-Halske-Ring 14, 03046 Cottbus, Germany

[6]Institute of Information Technology (Communication Electronics) LIKE, Friedrich-Alexander University Erlangen-Nürnberg (FAU), Am Weichselgarten 33 in 91058 Erlangen-Tennenlohe

[7]Department of Computer Science, Friedrich-Alexander University Erlangen-Nürnberg (FAU), Martensstr. 3, 91058 Erlangen, Germany

[8]Department of Computer Science, Friedrich-Alexander University Erlangen-Nürnberg (FAU), Martensstr .1, 91058 Erlangen

[9]Carl-Friedrich-Gauß-Fakultät, Technische Universität Braunschweig, Mühlenpfordtstraße 23, 38106 Braunschweig, Germany

[10]Heinz Nixdorf Institute and Dept. of Computer Science, Paderborn University, Warburger Str. 100, 33098 Paderborn, Germany

[11]Berlin-Brandenburg Institute of Advanced Biodiversity Research, Altensteinstr. 34, 14195 Berlin, Germany

*Correspondence: simon.ripperger@gmail.com

Abstract:

Recent advances in animal tracking technology have ushered in a new era in biologging. However, the considerable size of many sophisticated biologging devices restricts their application to larger animals, while old-fashioned techniques often still represent the state-of-the-art for studying small vertebrates. In industrial applications, low-power wireless sensor networks fulfill requirements similar to those needed to monitor animal behavior at high resolution and at low tag weight. We developed a wireless biologging network (WBN), which enables simultaneous direct proximity sensing, high-resolution tracking, and long-range remote data download at tag weights of one to two grams. Deployments to study wild bats created social networks and flight trajectories of unprecedented quality. Our developments highlight the vast capabilities of WBNs and their potential to close an important gap in biologging: fully automated tracking and proximity sensing of small animals, even in closed habitats, at high spatial and temporal resolution.

Keywords: wireless biologging network (WBN); ultra-low power; automated animal tracking; proximity sensing; bats; terrestrial biologging

Introduction

Recent advances in animal tracking technology have ushered in a new era in biologging[1, 2]. By collecting data of unprecedented quantity and quality, automated methods have revolutionized numerous fields including animal ecology[3], collective behavior[4], migration[5], and conservation biology[6]. For example, automated tracking of animals from space has advanced considerably over the past decade, in particular for observing large-scale movements[1]. However, satellite communication for localization or data access requires a lot of energy, and heavy transmitters greatly limit our ability to track smaller vertebrate species[1]. Efforts to further miniaturize increasingly powerful biologging devices culminated in the launch of the ICARUS initiative in 2019, which aims to achieve global animal observation at a small tag weight through a combination of GPS tracking, on-board sensing, energy harvesting, and energy-efficient data access from low space orbit[7]. ICARUS promises a great step forward in tracking large-scale movements such as migration. GPS tracking, however, is often not ideal or feasible for field biologists studying behavior on smaller spatial scales. GPS tracking of small vertebrate species is further limited by the considerable weight of GPS devices[1]. Satellite reception is hampered by complex habitats and impossible if animals go inside trees, caves, or underground burrows.

In industrial applications or for civilian surveillance, low-power wireless sensor networks (WSNs) fulfill requirements similar to those needed to track animal behavior at high resolution and at low tag weight[8]. Consistently, there have been numerous applications for WSNs in wildlife monitoring ('biologging') since the early 2000s[9]. In the last decade, more sophisticated approaches have created powerful monitoring systems, e.g., for high-resolution tracking[10] and fully automated logging of social encounters[11, 12]. The major challenge in developing efficient wireless biologging networks (WBNs) is to design ultra-low power communication networks in order to maximize performance, minimize energy consumption, and reduce tag weight.

Here, we describe a system that takes WBNs to the next level: a multifunctional and thus Broadly Applicable Tracking System ('BATS', Figure 1). We first present a solution for

direct proximity sensing that enables the collection of proximity data at a temporal resolution of seconds, at tag weights of one to two grams, and with runtimes of up to several weeks depending on the sampling rate. Second, we describe an adaptive option for triangulating spatial positions based on Received Signal Strength (RSS) by ground-borne localization nodes. This adaptive option allows automated recording of robust movement trajectories even in structurally complex habitats. Third, we explore a new, almost energy neutral solution for remote data access over distances of several kilometers at low data rates. Finally, we present an energy model that shows the effect of the parameter settings of software tasks on the runtime of the animal-borne tag. First deployments of BATS have resulted in proximity and tracking data of unprecedented quality and have demonstrated the high potential of WBNs for studying (social) behavior. Our developments highlight the vast capabilities of WBNs and their potential to close an important gap in biologging: fully automated tracking and proximity sensing of small animals, even in closed habitats, at high spatial and temporal resolution.

Results

The modular structure of BATS allows researchers to combine proximity sensing, long-range telemetry, and high-resolution tracking (Figure 1) depending on the research question and the behavior of the animals. We chose bats to test and validate the system since they are small-bodied and move fast in dense vegetation, both challenges to the performance of the WBN. Three recent field studies were conducted in temperate and tropical habitats on three bat species: greater mouse-eared bats (*Myotis myotis)*, common noctules (*Nyctalus noctula*) and common vampire bats (*Desmodus rotundus*). Each study documented high-resolution proximity data by direct proximity sensing among animals and automatically forwarding data to ground nodes (Figure 1a) that were deployed at roosting or foraging sites. Bat-borne mobile nodes that came within the reception range of the localization grid automatically increased their sampling rate to enable high-resolution localization (Figure 1b). Data for the synchronization of clocks was transmitted successfully over distances of more than 4 km by

long-range telemetry (Figure 1c). The following sections describe the empirical validation of the system.

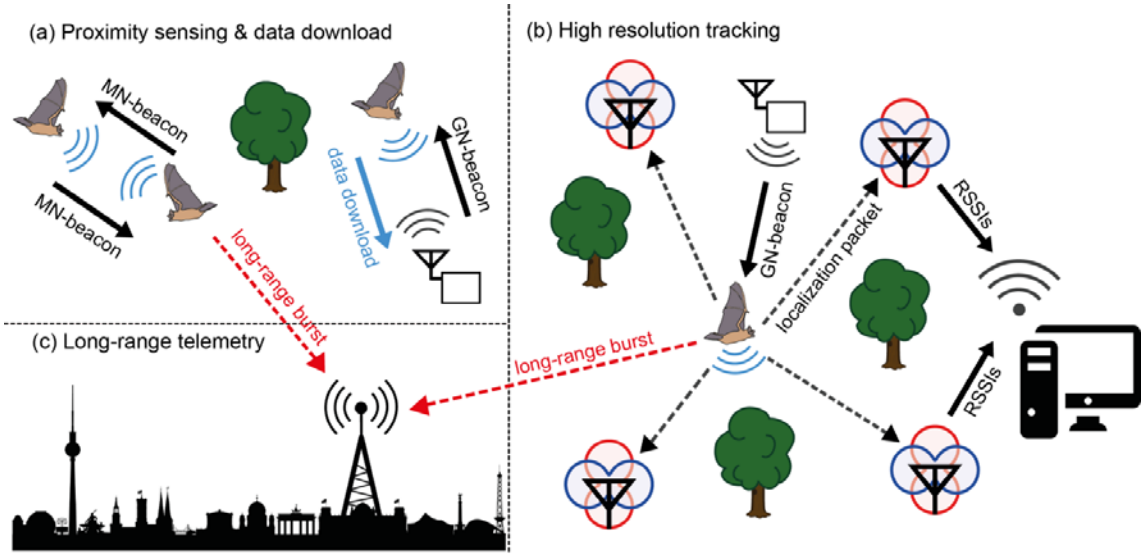

Figure 1: BATS overview. (a) Animal-borne mobile nodes (MNs) document animal-animal meetings, which are triggered by MN-beacons 24/7 and independently of ground infrastructure. Each mobile node forwards its meeting data when it receives beacons from a ground node (GN) that is dedicated to downloading and storing data. (b) When a tagged animal enters a grid of localization nodes (depicted by an antenna with red/blue gain patterns), a beacon of a tracking-dedicated GN triggers the transmission of localization packets from the MN to the localization nodes. Received signal strength indicators (RSSIs) of the impinging localization packets are then sent from the localization nodes to a work station via a WLAN. (c) Long-range bursts, which contain encoded sensor data, are received by long-range receivers. Long-range telemetry enables data transmission over distances of several kilometers at a low data rate.

High-resolution social network data from direct proximity sensing

Fifty individuals of one large natural colony of common vampire bats (*Desmodus rotundus*) were tagged simultaneously in Panama. Associations with other tagged bats are fluid and

highly dynamic both during day and night. For example, Figure 2a shows the course of the meeting history and the dynamic range of degree centrality for a single bat (ID 56) over a two-day period. The high temporal resolution of meetings (all mobile nodes in reach communicate with each other every two seconds) also makes it possible to infer a behavior such as departure from the roost or movement within the roost. For example, foraging bouts can be identified by a sudden drop in meeting partners at night, which can be verified by contacts to ground nodes outside the roost. Autonomous direct proximity sensing allows monitoring changes in roosting associations, caused by moving among subgroups within the roost (Figure 2b, c) and it also allows inferring 'social foraging networks' outside the roost (Figure 2d). In addition, every meeting is labeled with a maximum signal strength intensity indicator (RSSI). This makes it possible to subset the meeting dataset according to signal strength, an estimate for proximity[13]. RSSI values can distinguish close-contact associations from associations based on merely occupying the same area.

The social networks created from direct proximity sensing are independent of the whereabouts of the tagged bats and provide an adaptive temporal resolution of seconds. Almost 400,000 individual meetings were recorded during the first eight days of our field test. To take bats as an example, the typical approach for collecting social network data has been to sample some unknown portion of co-roosting associations in a sample of identified roosts each day[14]. Our system allows complete networks of all bats every few seconds. This temporal resolution makes changes in social gathering directly visible if time slices in high-resolution data are small enough[15]. We believe this represents an extraordinary advance for studying such small free-ranging animals, and it allows for an analytical depth which is so far known predominantly from human social networks generated by communication among smart phones or social media[15].

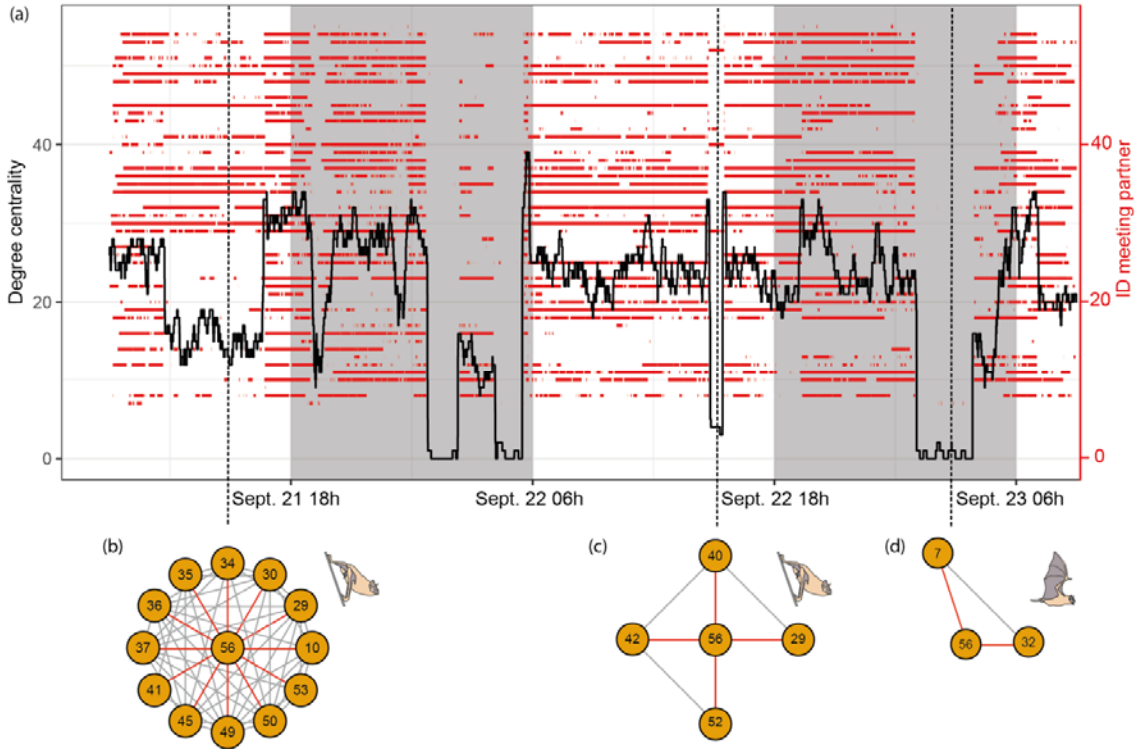

Figure 2: High-resolution association data in wild vampire bats. (a) Meeting history of a single vampire bat (ID 56; 50 tagged bats in total) with other tagged bats. Red lines show meetings between bat 56 and other tagged bats (right-hand y-axis). The black line shows the degree centrality (number of associated tagged bats, left-hand y-axis) of bat 56 every two seconds. Date and time are on the x-axis. Shaded areas indicate night time. Vertical dashed lines show egocentric social networks at each snapshot of time during roosting (b,c) and foraging (d). Associations with the focal bat are indicated by red lines.

RSSI-based localization from angle-of-arrival estimation:

Seventeen wireless localization nodes were used to track tagged 11 mouse-eared bats (*Myotis myotis*) over an area of approximately 1.5 ha in an old, natural deciduous forest in northern Bavaria (Germany, Forchheim). We were able to reconstruct flight trajectories from foraging mouse-eared bats. Figure 3b shows as an example two trajectories of one foraging mouse-eared bat during two different nights in early August.

We evaluated the spatial resolution of the tracking system by estimating a trajectory from a defined reference path using unscented Kalman filters. The reference path and

estimated trajectories are shown in Figure 3a. The trajectories were calculated from angle-of-arrival estimates of signals impinging on localization nodes. Angles were estimated from difference measurements of received signal strength (RSS) at two orthogonal antenna gain patterns. This procedure in combination with a set of post-processing techniques for probabilistic multipath mitigation makes the trajectories robust to multipath propagation. The calculated trajectory is based on 4,912 data sets, while one set was composed of up to 2x17 RSS difference measurements (one per frequency band), if all 17 localization nodes were within the reception range of the mobile node. For comparison, we also analyzed four tracks recorded by a 15 g heavy-duty Ornitela GPS tracker, which is commonly used for tracking large birds of up to 450 g body weight. The mean positioning error was 7.30 m for the Ornitela GPS tracker and 5.65 m for the trajectory of the BATS system.

We calculated the positioning accuracy at lower densities of the localization grid. Localization was less accurate with fewer localization nodes (Figure 4), but it was robust and comparable to the full tracking grid (17 nodes) when using 15 - 16 nodes. With 12 - 14 nodes, we observed increasing variation in average error rates. With 11 nodes, the mean error was similar to the results from GPS tracking. Variation increased steadily with lower numbers of nodes and the mean error reached more than 10 m with a maximum error rate of 34 m at 6 nodes. At such low grid densities, the localization results tended to diverge, resulting in increasing positioning errors. In addition, sparser grids lack robustness against multi-path scattering. Consequently, the node density may only be reduced to a certain point, while positioning errors remain quite stable (Figure 4).

These analyses show that 11 localization nodes over an area of 1.5 ha in a forested habitat might be sufficient to construct high-resolution trajectories comparable in quality to a heavy-duty GPS tracker, which would only last for a few hours using a 15 g device, or to reverse GPS in open desert habitats[10]. Only moderate resources and human effort are needed to cover an area of a few hectares. For example, a setup as described above consisting of 11 localization nodes is deployed and configured by two people in one to two workdays.

198

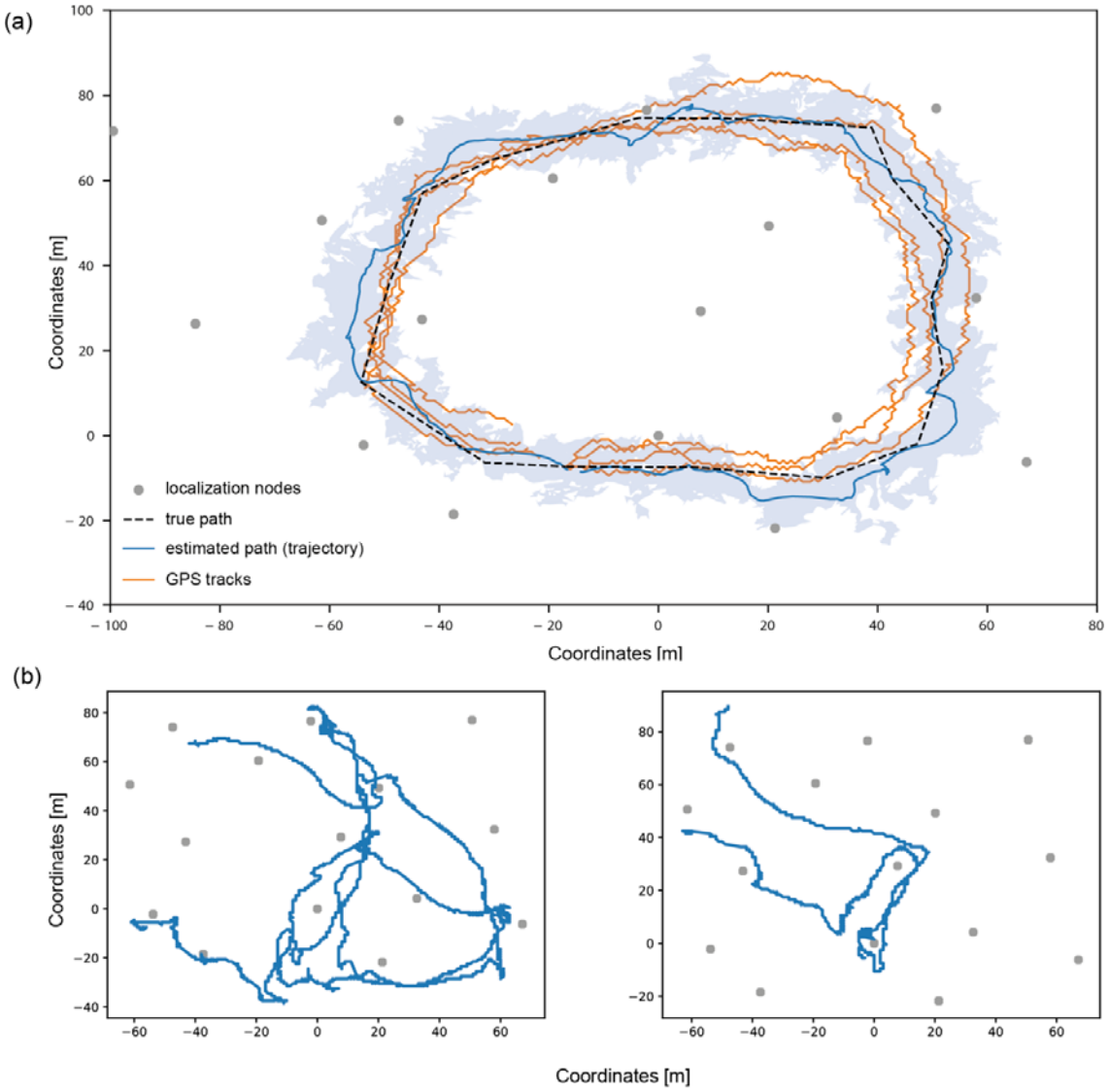

199

200 **Figure 3: Tracking bat movements in a forest.** (a) Tracking grid in a deciduous forest of

201 Forchheim, Germany, consisting of 17 localization nodes (grey dots) covering an area of ca.

202 1.5 ha. Dashed black line: known reference path; blue line and blue shading: estimated path

203 and average localization error obtained by BATS; yellow lines: four individual GPS tracks. (b)

204 Estimated flight trajectories of a tagged mouse-eared bat during foraging on August 2nd and

205 5th.

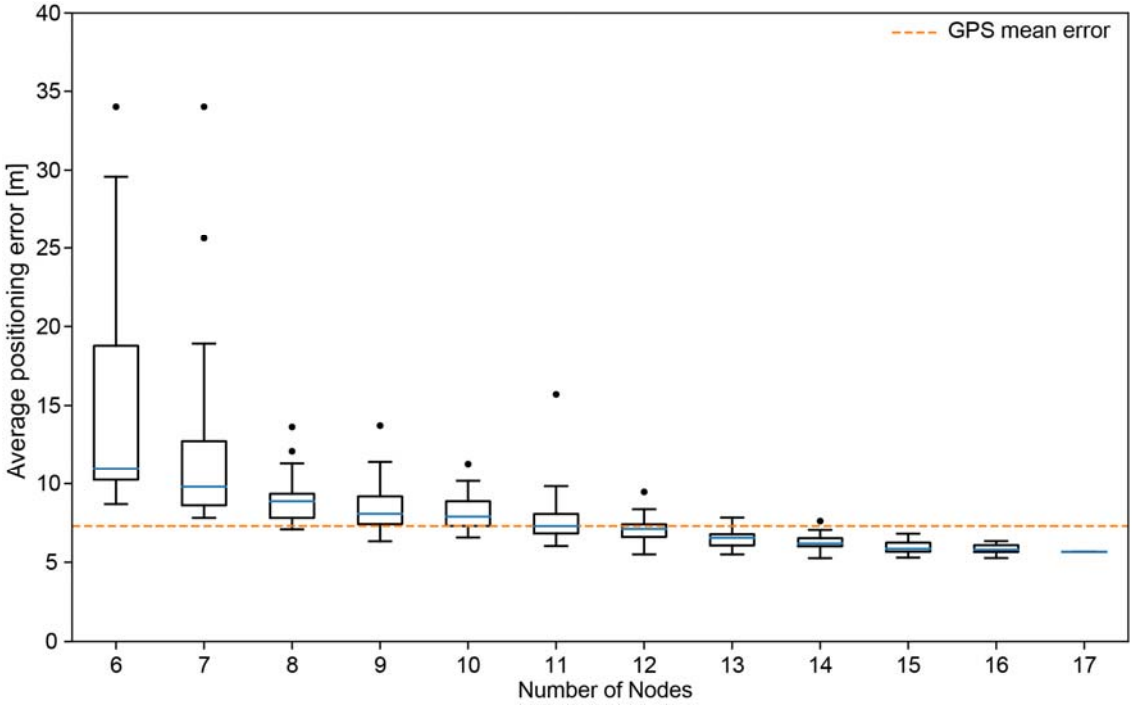

Figure 4: BATS tracking performance vs GPS tracking. Localization errors of a reference path of ca. 300 m by BATS are shown for different numbers of tracking nodes (6-17) in a deciduous forest of ca. 1.5 ha area. The average positioning error of four tracks of a heavy-duty commercial wildlife GPS tracker is shown for comparison by a yellow dashed line.

Distance verification of packet transmission by long-range telemetry:

Transmission distances of data packages were measured in an urban green area. 34 noctule bats (*Nyctalus noctula*) were tagged in a forest within the city of Berlin and two long-range telemetry receivers were placed at a distance of about 1 and 4 km from the forest.

Mobile nodes transmitted with each MN-beacon a burst for long-range transmission of the mobile node's time stamp. During a period of two weeks, we were able to receive more than 168,000 long-range bursts, which allowed us to successfully recover 9,511 complete timestamps from 32 individual bats. To mitigate the impairment by interfering transmission, one complete long-range telemetry packet is split over 24 single burst transmissions. At the long-range receiver, 24 subsequent bursts are merged to one actual long-range packet containing the ID and the bat's time reference. This transmit scheme assures that the mobile node's transmit module is only activated for a short time period avoiding stress on the

224 batteries and hardware. In addition, it avoids interference of other channels by a time-
225 frequency hopping pattern in transmission. Instead of a complete package loss, only a
226 fraction of the collection of bursts might be corrupted, which can be reconstructed by means
227 of error-correction codes at the receiver side. It is only due to this specialized telegram-
228 splitting technique[16] that a long-range transmission under extreme power-restrictions and
229 vastly occupied frequency channels becomes possible.

230 Reception of long-range data should perform best when the tagged bats move in
231 open airspace. However, we recovered a considerable number of these long-range bursts
232 while bats were inside their roosts during the day. 563 long-range bursts received during the
233 day were mapped to the known roosts of the bats, allowing us to measure the transmission
234 distance. Fifty-seven long-range bursts from four bats inside their roost were recovered over
235 distances of ca. 4.2 km (between roost 1 or 2 and the receiver at the cogeneration plant,
236 Supplementary Figure 1). 506 long-range bursts from five tagged bats were recovered at
237 distances between 667 and 819 m (between roost 1 or 3 and the receiver at the retirement
238 home, Supplementary Figure 1). Burst retrieval over distances of more than 4 km was
239 surprising. Theoretical calculations predicted transmission distances of about 5 km assuming
240 barrier-free transmission[17]. In the field, however, signals had to pass first through the wooden
241 wall of the tree roost and second the forest's vegetation, which should greatly reduce
242 transmission distance.

243 Data recovery is a major challenge in automated light-weight tracking-systems. Signal
244 transmissions inherently suffer from limited transmission power under heavy losses due to
245 distance, shadowing, and other interfering signals. Remote downlinks, e.g., per GSM (Global
246 System for Mobile Communications), add considerable weight in the form of circuitry and
247 battery[1]. Many light-weight trackers must therefore be retrieved, or energy harvesting must
248 be used to counter-balance the expenses for remote data download[7, 18-20], again adding
249 weight for the required hardware components. When tagged animals move on predictable
250 scales, energy-saving methods like transfer via VHF (Very High Frequency) or radio modems
251 may be an option to receive data over distances of hundreds of meters to few kilometers[21].

Our scenario explores options to decrease the energy expense for downloading stored data to a negligible proportion of the overall energy budget (compare Figure 5). For data download over short distances of ca. 100m, we accumulate and pre-process data on-board and use sophisticated communication protocols that maximize data-package reconstruction while minimizing energy demand[22, 23]. The above described long-range telemetry mode provides an option for robust transmission of small amounts of data at a low rate without the expenditure of additional energy due to the hybrid modulation of the signal. In comparison, other long-range systems for biologging, such as LoRa[12], enable higher transmission rates. However, the bi-directional communication between transmitter and receiver strongly increases the energy demand no the mobile node.

Sensor node energy consumption and lifetime

A major strength of WBNs is the ease of adjusting parameters such as sampling rate and in turn energy consumption. These adjustments can maximize runtime for a given battery capacity, or alternatively maximize sampling rate to obtain higher resolution data. To investigate the impact of the different software-task parameters on runtime, we derived a model for energy consumption. We computed examples of runtimes of mobile nodes for two battery capacities and different parameter settings (Table 1). For example, the increase in energy consumption when tracking two to four hours per day can be compensated by extending the MN-beacon intervals. We achieve runtimes of at least five days using a 12mAh battery (corresponding to a 1g mobile node) even at the shortest beacon intervals of two seconds (active mode) and with two hours of high-resolution tracking per day. Depending on the parameter settings, we achieve runtimes of up to 13 days using the smaller battery and 25 days using 22mAh (Table 1).

Table 1: Estimated runtimes of mobile nodes for two battery capacities of 12 or 22 mAh inferred by an energy model for MN-runtime. While the model comprises seven energy consuming tasks, the shown runtimes are based only on varying MN-beacon intervals

and localization time (i.e. animal is within the localization grid). For MN-beacon intervals two operation modes are possible, depending on whether an animal is within reception range of a ground node (inactive mode) or not (active mode).

MN-beacon interval [s]		Time inside tracking grid per day [h]	Estimated runtime [h] for a battery capacity of 12 / 22mAh
if absent from ground node (active mode)	if near ground node (inactive mode)		
2	10	0	151 / 278
10	30	0	321 / 589
2	10	2	135 / 248
10	30	2	257 / 471
30	60	4	247 / 454

Figure 5 illustrates the energy consumption of the different software tasks on the mobile nodes of the six different scenarios described in Table 1. When localization is disabled (i.e., only proximity sensing), sending out beacons to wake up other mobile nodes to initiate meetings strongly drives the energy demand (Figure 5a, b). Therefore, modifying the MN-beacon intervals has the highest impact on runtime. When localization is enabled, tagged animals send localization packages whenever they enter the tracking grid. The high duty-cycle of sending localization packages (8/s) strongly decreases the runtime (Figure 5c-e, Table 1). At active/inactive MN-beacon intervals of 2/10s, a daily localization period of two hours decreases the overall runtime by 10.8% (Fig 5 a, c, Table 1). At four hours of localization, the energy demand for localization dominates the overall energy consumption, in particular at high MN-beacon intervals.

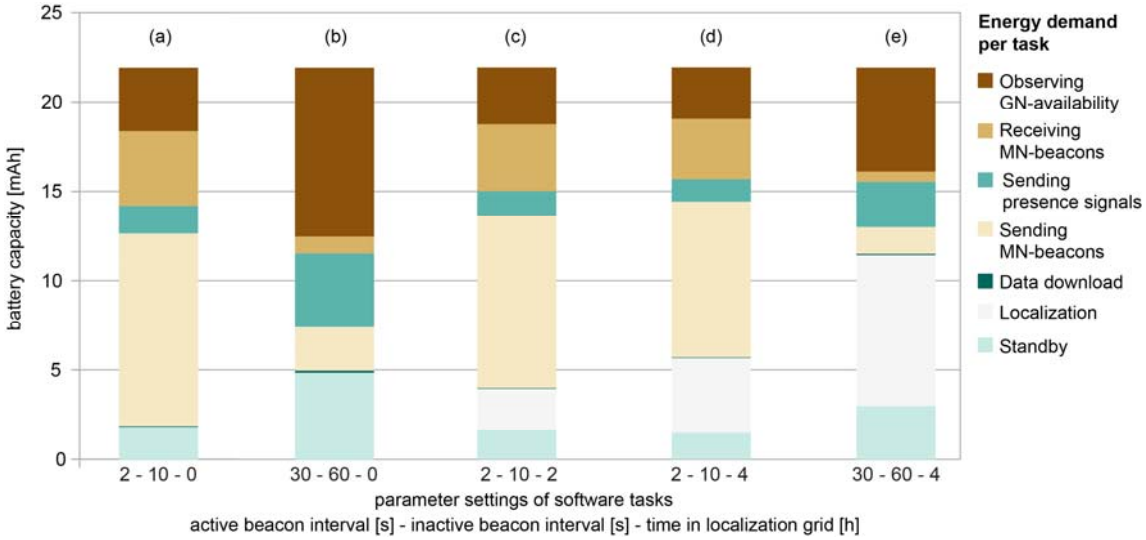

Figure 5: Energy distribution of software tasks of a mobile node powered by a 22mAh battery. Energy demand per software task depends on parameter settings for active/inactive beacon interval [s] and amount of time an animal spends in the localization grid [h]. The energy demand is shown for the seven major software tasks; MN = mobile node, GN = ground node. Zero time in the localization grid (a, b) refers to a pure proximity sensing scenario.

Model-derived runtimes were compared with empirical runtimes from field tests on noctule bats (*Nyctalus noctula*), where mobile nodes were either powered by a 12mAh battery or a 22mAh battery, resulting in MN weights of 1.1g to 1.9g depending on housing. The average runtime was 148h (max. 209h) for the small battery, while the model predicted 151h. For the larger battery, average runtime was 280h (max. 426h) with a predicted average value of 277h. For both batteries, the predicted values were very close to the observed (1.8% overestimation and 0.7% underestimation, respectively) indicating that the model is a reliable tool for experimental design of a field study.

Discussion

In past years, developments in high-performance proximity sensing using significantly larger animal-borne tags[24] and in ground-based high-resolution tracking in low-clutter desert

315 environments[10] have previously pushed the boundaries of what was technologically feasible.
316 BATS takes the next step by combining these functionalities while keeping the tag weight at
317 one to two gram. Adhering to the 5% rule[25], even animals weighing as little as 20g can be
318 tagged with this system. These smaller species make up a large proportion of birds and
319 mammals (see Figure 3 in[1]) and WBNs will give researchers new capabilities to address a
320 wide range of questions in animal behavior and ecology. Our adaptive and scalable system
321 design provides great flexibility to tailor such a system, allowing adjustable use for any
322 species- and study-specific requirement. The design of the mobile node allows to add
323 multiple functionalities beyond the ones presented here, such as accelerometers,
324 magnetometers, or even an on-board electrocardiogram (ECG) sensors[26].

325 An early example of automated tracking of small-bodied animals on a limited
326 geographic scale was ARTS, a system for automated VHF tracking, which was installed on
327 Barro Colorado Island, Panama[27]. This six-year endeavor in the 2000s already highlighted
328 the promising opportunities offered by WBNs: scalability, remote reconfiguration, full
329 automation, and low-cost tags. Yet, a rather low positioning accuracy (~50 m) and restricted
330 coverage were limiting factors[27]. Most of today's solutions for automated tracking of small
331 animals such as songbirds, bats, or rodents perform best at larger geographic scales or in
332 open habitats. For example, current versions of 1 g GPS loggers are suitable to explore
333 seasonal large-scale movements[18, 20]. However, they cannot reconstruct flight paths in a
334 complex environment, since they can only collect around 100 fixes. Furthermore, the
335 physical devices must be retrieved for data recovery, and satellite reception suffers within
336 vegetated areas. Alternatively, reverse GPS can track small animals much more energy-
337 efficiently and at much higher temporal and spatial resolution by measuring time-of-flight at
338 ground-based receiving stations[10]. However, time-of-flight measurements are inherently
339 affected by vegetation and perform best in open areas. Therefore, we combined signal
340 strength measurements (including angle of arrival (AoA) estimates) from two frequency
341 bands and probabilistic multipath mitigation[28] to create a system that is robust to multipath
342 propagation and thus performs well in complex environments. Common but costly measures

to resolve multipath propagation are large-aperture antenna arrays for AoA tracking or large signal bandwidth for time-of-flight tracking. However, the future of animal tracking will most certainly center on low cost, ultra-low power integrated circuits, which are currently experiencing a noticeable push due to their broad applications in Industry 4.0 and 5G. This technology has the potential to dramatically boost the capabilities of biologging devices.

Contact networks of small-bodied animals have received increased attention in past years and are most commonly built from RFID- (radio-frequency identification) or PIT- (passive integrated transponder) tagged animals that were observed to be feeding or sleeping at the same site at the same time[29-31]. Later developments for direct encounter logging were able to log association independently of the locality. However, these sensors were either quite large and heavy[11] or had short runtimes of less than 24h[32] due to the high energy demand for the permanently active receiver — a major shortcoming for applications in small-bodied species. We show that the use of wake-up receivers and adaptive operation paired with novel wireless communication protocols dramatically reduce the energy demand of such wireless sensor tags. We believe that direct encounter logging or more precisely proximity sensing will enable diverse research in the future, as this approach creates large datasets, with additional sensor data providing the behavioral context closing the gap between social patterns and their underlying processes[2].

Ongoing work on ultra-low power sensor networks not only targets animal tracking systems but a variety of "Internet of Things"-solutions in general. Energy efficiency is not only a question of hardware circuit design but also of how to interact across all relevant layers in the node's software stack (i.e., application, and operating system). On the mobile node, the interaction aspect between communication layers (e.g., application and MAC layer) concerns the placement of certain functions (e.g., retransmissions) within the entire software hierarchy[33] such that energy-efficient operation is not affected by unnecessary functional redundancies. Besides, cross-layer designs that optimize the timing of communication processes and make them deterministic at least within limits[34] form the software-engineering basis for an overall energy-aware systems approach. In our scenario, energy-efficient and

371 reliable communication between nodes are cross-cutting concerns, since failed
372 communication attempts lead to additional overhead for retransmissions. Very promising
373 examples for low-power communication initiation are novel selective wake-up receivers[35],
374 which allow the small tags to enter sleep modes in the nano-ampere range rather than
375 constantly operating in the micro- or milli-ampere range. Selective wake-up concepts allow
376 waking up dedicated recipients of a message (or a selected subset thereof) instead of
377 waking up all systems in communication range. Integrated into the animal tracking nodes,
378 this could enable the next quantum leap on low-power operation. The alternative to making
379 the receiver operate on a lower energy budget is to make the communication more reliable.
380 Recent advances in integrating coding for forward error correction into such lightweight
381 systems show very promising results, e.g., using erasure codes[22]. Ultra-reliable
382 communication protocols currently used in 5G networks can also be applied to localization
383 nodes, which are used for quasi-live tracking in the bat tracking scenario. For example, the
384 ground network can be used as a distributed antenna array, which allows the use of smart
385 decoding algorithms for very weak communication signals to further optimize data recovery[36].
386

387 **Conclusions**

388 There is no single best method for tracking animal behavior. RFID- and PIT-tags allow
389 monitoring presence of animals at known sites at low cost. Satellite-based localization will
390 remain the method of choice to monitor large-scale movements such as migration or to
391 explore unpredictable events such as nomadism[1, 37]. However, we believe that WBNs like
392 BATS will greatly benefit biologging of small animal species that move over smaller and more
393 predictable spatial scales, especially inside of habitats where signal transmission is
394 constrained. The homologies of applications between mobile communications and biologging
395 (e.g., Bluetooth low energy for communication among mobile nodes[12]) will boost the
396 development of WBNs. Experimental setups including automated triggers (e.g., acoustic
397 playbacks or other sensory cues) might easily be integrated and direct proximity sensing will
398 bring exciting research opportunities. Such setups will allow to study the effect of social

399 network dynamics on phenomena such as transmission of social information[30] and
400 pathogens[38], and key ecosystem functions such as pollination and seed dispersal[39].
401
402 **4. Methods**
403 *The* WBN *hardware, software, and functionality:*
404 Figure 1 is a schematic overview of BATS. In order to study its performance, we empirically
405 evaluated the three major functions of the system: proximity sensing (Figure 1a), high-
406 resolution tracking at local scales (Figure 1b), and long-range telemetry (Figure 1c). See
407 Glossary (Supplementary Table 1) for definitions of terms.
408
409 *Proximity sensing:*
410 Any given mobile node (MN) dyad generates meetings whenever it comes within reception
411 range (5 - 10 m depending on the environment). The animal-borne MN consists of a 22mm x
412 14mm Flex PCB circuit board, which is populated with a central System-on-Chip (EFR32,
413 Silicon Labs) containing an ARM Cortex-M4 core and two radio frontends for 868/915MHz
414 and 2.4GHz (Supplementary Figure 2). The transmitter in the sub-GHz frontend periodically
415 sends MN-beacons, a signal that contains a wake-up sequence. The rate of beacons is
416 configurable (see below). A low-power wake-up receiver on the MN triggers the conventional
417 receiver to receive incoming information on the ID whenever a MN-beacon is received from
418 another MN. Subsequently, a meeting is created between the communicating MN-dyad
419 (Figure 1a left). While a conventional receiver draws a relatively high current in receiving
420 mode waiting for incoming packages, a wake-up receiver achieves this functionality with a
421 low current (yet, at cost of sensitivity and performance). When no further MN-beacons are
422 received from the meeting partners for 5 MN-beacon intervals, the meeting is closed and
423 stored to memory along with the ID of the meeting partner, meeting duration, maximum RSSI
424 and a relative timestamp. The mobile node contains both persistent and volatile random-
425 access memory for data storage.

426 The conventional receiver of the sub-GHz frontend is periodically activated to observe
427 the presence of a ground node (at a fixed interval of every two seconds), which is indicated
428 by a ground node beacon (GN-beacon), periodically broadcast by the transmitter of each
429 ground node (Figure 1a right). The transmitter supports several configurations defining the
430 main purpose of the ground node (GN) and enabling location-dependent adaptive operation
431 of the WBN. (i) A download-dedicated GN broadcasts a signal that enables transmitting MN
432 data based on a customizable RSSI threshold received at the mobile node. (ii) A tracking-
433 dedicated ground node positioned within the grid of localization nodes for high-resolution
434 tracking broadcasts a signal that activates the 2.4GHz frontend in addition to the sub-GHz
435 front end on the MN, transmitting 'localization packets' at a rate of 8 packets per second. (iii)
436 A presence-detection-dedicated GN triggers the transmission of 'presence signals' by an MN
437 and stores incoming signals which can be used to determine presence/absence of tagged
438 individuals (presence at resources or at sleeping sites). Combinations of functionalities (i-iii)
439 may be used in a single GN if desired (e.g., a tracking-dedicated GN can also trigger data
440 download). Incoming MN data is received by the GN and stored by a Raspberry Pi
441 (Raspberry PI Foundation, Cambridge, UK) to a SD card along with the ID of the transmitting
442 MN and the receiving GN, respectively, and a timestamp, which is provided by a GPS unit.
443 The Raspberry Pi also hosts a WiFi allowing the user remote data access.
444 Visualization of proximity sensing data is facilitated by the custom-made software
445 'meeting splitter' (see Figure 2). For each specified mobile node ID, the current meeting
446 partners are projected onto a discrete time axis (one second resolution). We specified a
447 configurable time window around each point on the time axis (five seconds in case of Figure
448 2). All ongoing meetings, which overlap with the window around the respective point in time,
449 are included in the set of associated bats at this particular point in time. The result per bat is
450 a set of associated bats per each second in the dataset. A subsequent automated analysis
451 classifies each meeting as inside or outside the roost, depending on the number of
452 simultaneous meeting partners (not applied in this manuscript).
453

RSSI-based high-resolution tracking:

Localization nodes (LN) perform field strength measurements, which are collected by WLAN and are processed by a PC including a file system whenever animal-borne mobile nodes enter the localization grid (Figure 1b; localization nodes collect localization packets from mobile nodes; the transmission is triggered by a ground node). Each localization node comprises a software-defined radio (consisting of a radio-frequency frontend, a highly integrated analog-to-digital converter, a field-programmable gate array and a microcontroller) and two receiving antenna gain patterns each with two main lobes (Figure 1b, red and blue pattern, respectively). The bi-lobed shape indicates the directional sensitivity of the antenna, while the direction of each lobe represents its maximum in sensitivity. The red pattern is rotated by 90° compared to the blue pattern, and both are simultaneously used to estimate the angles of arrival (AoA) of the localization packages transmitted by the animal-borne MNs. The difference in received signal strength (RSS) of the two patterns relates to AoA: If the difference – RSS of the blue pattern minus RSS of the red pattern – is maximum, the wave front impinges on the localization node either from east or west; if the RSS difference is minimum, the direction of arrival is N or S. Accordingly, there are four options for the AoA if the difference is zero: NE, NW, SE or SW. These ambiguities are resolved by fusing measurements of several localization nodes.

This design allows us to exploit not only error-prone absolute field strength measurements[40], but also fail-safe angles of arrival. These are not affected by faulty propagation laws or shadowing effects, because both error sources disappear when forming the RSS differences. The angular resolution of the AoA estimates improves with increasing ambiguity of the antenna pattern designs. However, more localization nodes have to be in reach to resolve the ambiguity[41]. During the Forchheim field trial, we collected up to 272 angle estimates per second when all 17 localization nodes were in reception range.

To further improve localization accuracy, we exploited three sources of information ((a) model-based Bayesian positioning, (b) frequency diversity, (c) retrodiction), which increase robustness against multipath propagation. This effect complicates the positioning

process, in particular in structurally complex environments since wave fronts impinge a localization node out of the different directions of multiple reflectors (e.g., surrounding vegetation). The information sources to counteract multipath-related adverse effects are described in the following:

(a) Model-based Bayesian positioning: Due to the nature of multipath propagation, a stochastic model can be devised to characterize the resulting spread in the AoA estimates[28]. This AoA measurement model can be incorporated into the likelihood function of the recursive Bayesian positioning process, e.g., based on a Kalman filter or a related grid-based estimation filter[42]. The recursive estimation process yields a probability distribution characterizing where the bat may be, considering propagation characteristics from a local channel model[43]. All measurements are fused during the recursive process taking into account a movement model reflecting the flight characteristics of a bat (e.g., max. flight speed). The better the agreement of the various AoA estimates, the more pronounced the positioning probability distribution.

(b) Frequency diversity: Multipath propagation leads to frequency-dependent fading. We therefore measured field strength not only on the primary far-reaching carrier frequency at 868 MHz, but also on a secondary carrier frequency at 2.4 GHz. On both carrier frequencies, wave forms comprising several subcarriers are employed to enhance the field-strength based AoA estimation process. Due to the large carrier frequency separation (> 1.4GHz), frequency-dependent fading effects are de-correlated even if multipath time-of-flight differences are minor, i.e., in the range of a few meters, which corresponds to our accuracy level.

(c) Retrodiction. If we do not have to estimate the position of a particular bat in real-time, we can exploit all measurements of a bat to estimate a complete trajectory. Forward-backward filtering enhances estimation quality considerably, yielding a positioning quality in the range of 4 m (1 - σ). Performance limits of field-strength based positioning have been discussed in depth[41, 44].

We evaluated the trade-off between tracking grid density and localization quality for the Forchheim setup, which comprised 17 localization nodes. In particular, we asked: how many localization nodes are required to obtain localization quality comparable to heavy-duty GPS tracking? We selected subsets of 6 to 16 out of the 17 localization nodes in order to observe the decrease in positioning accuracy with decreasing grid density. Trajectories including standard deviation were estimated for each subset of localization nodes. 17 configurations were calculated for the grid consisting of 16 nodes (all possible subsets of the full grid) and 25 unique, randomly chosen subsets for all remaining grid configurations (6 to 15 nodes, respectively) to obtain average errors for the given number of nodes (see Figure 4).

Long-range telemetry

Our long-range telemetry approach aimed at transmitting long-range bursts from mobile nodes over distances of up to several kilometers – much longer distances than our download-dedicated ground nodes would allow for – within the city of Berlin, under harsh shadowing by obstacles (vegetation, buildings, etc.) or in presence of numerous interferes. We periodically transmitted 'long-range bursts', i.e., relative timestamps in form of seconds since mobile node start-up generated by a simple clock counter. These timestamps are crucial for post-processing of meeting because they allow accounting for clock drift on the mobile node. We embedded the long-range functionality into the existing modulation scheme using a hybrid phase-alternating modulation on top of the pure amplitude-modulated wake-up sequences of the MN-beacon[45]. As a consequence of the extreme energy limitation of the MN, we ensured the required Signal-to-Noise-Ratio (SNR) by counterbalancing the rate and the desired transmission distance. The combination of the hybrid modulation, the channel encoding procedure[17, 45] and the 'Telegram-splitting' technique[16] enables an ultra-low power long-range transmission without additional expenditure of energy. The long-range bursts were received at two long-range receivers, which were deployed on exposed sites (rooftops) at distances of ca. 200 - 1,800m (retirement home) and 3,300 - 4,500m (cogeneration plant;

see Figure S1) to the proximate respectively ultimate border of the urban forest where the roosts of the tracked bats were located.

We quantified communication distances in the field, which was possible when a tagged bat occupied a known roost and was simultaneously received by the long-range receiver. We therefore matched timestamps of signals received simultaneously by GNs at roosting sites and at long-range receivers. In case of a match, we quantified the distances between roosts and long-range receivers in the R package geosphere using the Haversine function[46]. The empirically assessed communication distances have then been compared to a theoretical model of long-range transmission distances[47]. This model evaluates achievable rate and distance of transmission based on the energy relation of the SNR, presuming the transmission power given by the MN's hardware configuration and a desired target payload rate. For simulating the channel characteristics faced by the MN, the model comprises parameters like the path loss in dependence of the signal-center frequency, the transmission distance and receiver and transmitter heights. Environmental influences like attenuation by obstacles, multi-path propagation or unpredictable rotation of the MN's rod antenna are incorporated by means of a random variable, stating the superimposed attenuation effects. Based on these assumptions we were capable of overcoming path losses of over 150dB for a distance of 5 km and more, under reasonable rates of packet loss[17], thus accomplishing an ultra-robust implementation supporting payload data rates of a few bits per second.

Sensor node energy consumption and runtime

A crucial aspect for biologging is knowledge on the runtime of the sensor nodes. Static program-code analysis methods of the mobile node are able to determine upper bounds on the nodes' runtime[48]. However, in the context of the BATS tracking system, precise estimates for the average uptimes of the system proved to be more beneficial for the empirical studies than upper bounds for the lifetime. Consequently, we focused on an energy model to determine the average runtime of the mobile nodes, which is strongly dependent on the tasks executed by the software. Our models are based on measurements of each executed task in

565 combination with empirically determined activity parameter of each task. That way, we
566 ensure highest accuracy for our model. In our setting, seven different tasks are implemented:
567 (i) Standby, (ii) sending MN-beacons, (iii) receiving MN-beacons, (iv) observing ground node
568 availability, (v) transmitting data to a ground node, (vi) sending localization packets, and (vii)
569 sending presence signals (see Table S Glossary for definition of terms).
570
571 We determined the runtime by using the specific energy demand for a task and by translating
572 it to an average current draw. With the average current draw and a given battery capacity,
573 the runtime can be computed as follows:

$$T_{runtimeavg} = \frac{E_{battery} \cdot \eta_{DCDC}}{\sum I_{tasks}}$$

574
575 ŋDCDC represents the efficiency of the DCDC-converter, which is permanently active and
576 consumes energy. Determining ŋDCDC is impractical, because it highly depends on the
577 actual current drain of the application for the entire runtime. For this reason, we assume a
578 fixed efficiency of 0.95, which translates to only 95% of the battery capacity being available
579 for software tasks. This way, losses caused by the DCDC and parasitic discharges of the
580 battery are modeled in a coarse-grained manner.
581 The idle current during standby is given in a current draw, which does not require any
582 further calculations. The other tasks (e.g., observing GN availability, sending localization
583 packets) are executed in predefined cycle times (duty cycle). Based on the measured energy
584 demand and the duty cycle, we calculated an average current draw for each task. The
585 energy demand for each task was measured in the lab with an Agilent DC power analyzer
586 precise source meter. In the case of a localization packet, which is sent every 128ms, the
587 average current draw can be expressed as follows:
588

$$I_{localization} = \frac{E_{localizationpacket}}{T_{dutycycle} \cdot V_{supply}} \cdot \frac{T_{localization}}{T_{day}}.$$

589 The average time spent inside the localization grid ($T_{localization}$) per day is strongly dependent
590 on the species-specific animal behavior and the experimental design. For the calculations
591 presented here, we set the daily localization period to 2 or 4 hours, respectively.

592 Observing a ground node in receiving range is carried out at a fixed duty cycle of 2
593 seconds. Here, the task is independent of the behavior of the tracked animal and the energy
594 demand is calculated as follows:

$$I_{basestationRX} = \frac{E_{basestationRX}}{T_{dutycycle} \cdot V_{supply}}$$

595 The transmission rate of MN-beacons and presence signals is adaptive based on the contact
596 to a ground node (i.e., a mobile node near a GN at a roost will decrease the duty cycle in
597 comparison to a MN on a foraging animal which is not in reception range of a GN). In turn,
598 the energy demand for sending beacons and presence signals highly depends on the
599 behavior of the tracked study species and the individual animal (e.g., time spent near GNs at
600 roosting sites). We therefore used empirical data obtained in the Berlin field test to inform our
601 energy model with realistic averaged parameter values for duty cycles of each task and the
602 amount of transmitted data. We quantified the average time-tagged bats spent in reception
603 range of a GN (inactive mode, decreased duty cycle) versus the time bats spent outside the
604 reception range of any GN (active mode, increased duty cycle). The common noctule bats in
605 the Berlin field test spent on average 47% of the observation time in the inactive mode and
606 the energy demand for transmitting beacons and presence signals calculates as follows:

$$I_{beaconTX} = \frac{E_{beaconTX}}{V_{supply}} \cdot \left(\frac{r_{\frac{inactive}{active}}}{T_{inactive}} + \frac{1 - r_{\frac{inactive}{active}}}{T_{active}} \right)$$

607

$$I_{presenceTX} = \frac{E_{presenceTX}}{V_{supply}} \cdot \frac{r_{\frac{inactive}{active}}}{T_{inactive}}$$

608

609 Receiving a MN-beacon depends on the duty cycle at which beacons are transmitted and on
610 the number of mobile nodes in receiving range. During the Berlin field test, we calculated the
611 average number of 2.05 maximum parallel meetings.

$$I_{beaconRX} = \frac{E_{beaconRX} \cdot N_{avgEncounter}}{V_{supply}} \cdot \left(\frac{r_{\frac{inactive}{active}}}{T_{inactive}} + \frac{1 - r_{\frac{inactive}{active}}}{T_{active}} \right)$$

612

613 For data download to a GN, we assumed static energy consumption (the energy demand for
614 sending a data packet highly depends on the size of the packet to be transmitted[23]. The
615 number of data packets to be transmitted is again dependent on the behavior of the tracked
616 animal (depending on how many meetings an individual accumulates). Mobile nodes on
617 common noctule bats sent on average 23.7 packages per hour to a ground node. Thus the
618 current draw can be denoted as:

$$I_{download} = \frac{E_{packet} \cdot N_{packetsperhour}}{3600s \cdot V_{supply}}$$

619 Based on these calculations, we matched the estimated average runtimes to the observed
620 runtimes during the Berlin field test (based on the last beacon or packet received from each
621 individual tagged bat).

622

623 *Adaptive operation, scalability, and reconfiguration:*
624 The adaptive operation contributes to the energy efficiency of BATS. We define location-
625 specific communication schemes on the mobile nodes which are initiated by ground nodes.
626 At a noctule bat day roost, for example, GNs activated the inactive beacon interval where
627 MN-beacons for meeting generation were only sent every 10 seconds. When tagged bats
628 leave their roost and move beyond the reception range of the GN, the MN switches to the
629 active interval, sending a MN-beacon every two seconds, which increases the probability to
630 detect also very short meetings in comparison to the inactive rate. Similarly, localization
631 packets, which strongly increase the energy demand, should only be sent when the tagged
632 animal moves within the tracking grid and are therefore triggered by a GN within the grid.
633 BATS tracks multiple individuals simultaneously. Our current design allows for the
634 observation of up to a theoretical maximum of 60 individuals. Field deployments containing
635 11 to 50 tagged bats empirically validated this targeted scalability. The scale of the

636 localization grid can be adapted to the ranges required for experimental setups. While we
637 tracked mouse-eared bats on 1.5ha, smaller areas might be sufficient to track, e.g., rodents
638 (bank voles, which showed a density of 40 - 162 individuals per hectare, have been tracked
639 on less than 0.5ha using automated VHF telemetry[49]). Tracking grids larger than 1.5ha are
640 certainly possible from a technological point of view. Yet, one has to keep in mind that effort
641 for maintenance (e.g., replacing power sources for localization nodes) scales with the size of
642 the tracking grid.

643 Since settings for communication schemes are sometimes difficult to pick a priori, we
644 built an option for reconfiguration of so-called 'soft-settings' (active/inactive rate of MN-
645 beacons, RSSI-thresholds for data download, localization interval, or timeout duration after
646 which a running meeting is terminated, etc.). Four values for every soft-setting (e.g., active
647 rate 2s, 4s, 10s, 30s) can be defined a priori and during operation ground nodes can be used
648 to trigger a switch between these pre-defined values at the mobile node.

649

650 *Field deployments*:

651 BATS functions as a modular system and hardware setup and software configurations are
652 easily tailored to a specific use case. We evaluated BATS during three major field studies by
653 applying mobile nodes to vampire bats, noctule bats, and mouse-eared bats with body
654 weights of 27 - 48g, 18 - 35g, and 22 - 28g respectively. While at least two of the three major
655 functionalities (proximity sensing, high-resolution tracking, long-range telemetry) have been
656 used in all three field studies, we focus on one specific functionality per deployment.

657

658 *Proximity sensing in vampire bats*:

659 We tagged 50 common vampire bats (*Desmodus rotundus;* 44 adult females, 6 subadults)
660 from a colony roosting in a cave tree near Tolé, Panama, to document social networks with
661 high resolution. Field work was conducted during September and October 2017. Mobile
662 nodes were powered by a 22mAh LiPo battery and housed in a 3D-printed plastic case,
663 resulting in a total weight of 1.8g. One download-dedicated ground node was positioned

664 inside the roost and five ground nodes were placed on surrounding cattle pastures to detect
665 the presence of foraging or commuting bats.
666
667 *Long-range telemetry in noctule bats:*
668 We captured and tagged 34 common noctule bats (*Nyctalus noctula*; 19 adult females and
669 15 juveniles) from two bat boxes in a nursing colony an urban forest in the city of Berlin,
670 Germany ('Königsheide Forst')[50]. Mobile nodes were powered by either a 12mAh or a 22mAh
671 battery and were housed either in a 3D-printed plastic case or in a fingertip of a nitrile lab
672 glove that was sealed with glue. Total weight varied between 1.1 - 1.9g depending on
673 housing and battery. We positioned 5 ground nodes underneath known roosts to document
674 the presence of individual bats and to remotely download data. In addition, we set up two
675 long-range receivers to evaluate model-based predicted data retrieval over distances of up to
676 4-5km[17]. This opportunity is particularly valuable to retrieve data of tagged individuals that
677 moved to an unknown roost.
678
679 *High-resolution tracking of mouse-eared bats*
680 We captured 11 mouse-eared bats (*Myotis myotis*) using mist-nets set up at ground level in a
681 mature deciduous forest near Forchheim, Germany. When hunting for ground beetles,
682 mouse-eared bats are faithful to their foraging sites for consecutive days. We therefore mist-
683 netted bats at an attractive foraging site rather than catching them from a roost in order to
684 track repeated bouts by returning individuals over the course of several days. Mobile nodes
685 were powered by 22mAh batteries and housed in fingertips of nitrile lab gloves (total weight
686 1.4g). At the capture site we installed a tracking grid consisting of 17 localization nodes
687 covering roughly an area of 1.5ha (see Figure 3). Distance between tracking stations varied
688 between ca. 25 - 40m. The irregular configuration was due to the presence of thick trees. We
689 aimed at positioning tracking stations at least 3 - 5m away from trees to reduce shielding of
690 the signal. We set up a polygon-shaped reference path for estimating localization errors and
691 determined the true position of the corners using a Leica Robotic Total Station TS16

692 (positioning error < 5cm). Corners were connected using strings, and we walked either a
693 sensor node (once) or a GPS tracker (four times) (Ornitela OrniTrack-15; a 15g solar
694 powered GPS-GSM/GPRS tracker; maximum logging rate 1 fix per second at a lifetime of ca.
695 4h without solar harvesting) along the calibration path and calculated the average localization
696 error based on the obtained tracks.
697
698 *Ethics*
699 Work on vampire bats: All experiments were approved by the Smithsonian Tropical Research
700 Institute Animal Care and Use Committee (#2015-0915-2018-A9 and #2017-0102-2020) and
701 by the Panamanian Ministry of the Environment (#SE/A-76-16 and #SE/AH-2-17).
702 Work on noctule bats: All necessary permits were obtained from SenStadtUm (I E 222/OA-
703 AS/G_1203) and LaGeSo (I C 113-G0008/16).
704 Work on mouse-eared bats: All experiments were approved by the government of Upper
705 Franconia (55.1-8642.01-15/13) and by the government of Lower Franconia (55.2-DMS-
706 2532-2-181).
707
708 **5. Acknowledgements**
709 This study was funded by grants of the Deutsche Forschungsgemeinschaft (FM, AK, RK,
710 KMW, WSP, JT, JR, FD) within the research unit FOR-1508, a Smithsonian Scholarly
711 Studies Awards grant (RAP, GGC, SPR, FM), and a National Geographic Society Research
712 Grant WW-057R-17 (GGC). We thank M Mutschlechner, M Nabeel, J Blobel, and M Hierold
713 for their contributions within the scope of the research unit. We highly appreciate logistical
714 support during the Forchheim field study by Naturstrom, MTS Meixner Transporte + Service,
715 C. Kreul GmbH & Co. KG, Spedition Pohl GmbH & Co. KG, and Siedlergemeinschaft
716 Lichteneiche. We are grateful to J Berrío-Martínez, D Josic, M Nowak, G Cohen, L Günther,
717 H Wieser, C Rüstau, B Peiffer, M Hammer, F Oehme and his BUND group of volunteers for
718 their support during field work. We express our particular thanks to J and C Mohr, who have

substantially contributed to the success of our field work. We thank E. Siebert for making the line work of *D. rotundus*.

Author contributions

SPR and FM conceived the ideas and designed the biologging studies; ND, BC, MH, TN, PW, and MS developed and tested the tracking technology; SPR, GGC, ND, BC, MH, TN, and MS collected the data; MH, TN, MS, SH, BC, PW and SPR analyzed the data; SPR led the writing of the manuscript. SPR, GGC, RAP, AK, RW, JT, JR, KMW, WSP, RK, FD, and FM contributed to acquiring funds. All authors contributed critically to the drafts, gave final approval for publication and agree to be held accountable for the work performed therein.

References

1. Kays, R., Crofoot, M.C., Jetz, W. & Wikelski, M. Terrestrial animal tracking as an eye on life and planet. *Science* **348**, aaa2478 (2015).
2. Krause, J. et al. Reality mining of animal social systems. *Trends Ecol. Evol.* **28**, 541-551 (2013).
3. Wilmers, C.C. et al. The golden age of bio-logging: how animal-borne sensors are advancing the frontiers of ecology. *Ecology* **96**, 1741-1753 (2015).
4. Hughey, L.F., Hein, A.M., Strandburg-Peshkin, A. & Jensen, F.H. Challenges and solutions for studying collective animal behaviour in the wild. *Philosophical Transactions of the Royal Society B: Biological Sciences* **373**, 20170005 (2018).
5. McKinnon, E.A. & Love, O.P. Ten years tracking the migrations of small landbirds: Lessons learned in the golden age of bio-logging. *The Auk* **135**, 834-856 (2018).
6. Fraser, K.C. et al. Tracking the conservation promise of movement ecology. *Frontiers in Ecology and Evolution* **6**, 150 (2018).
7. Curry, A. The internet of animals that could help to save vanishing wildlife. *Nature* **562**, 322 (2018).
8. Oppermann, F.J., Boano, C.A. & Römer, K. in The Art of Wireless Sensor Networks 11-50 (Springer, 2014).

748 9. Juang, P. et al. Energy-efficient computing for wildlife tracking: design tradeoffs and early
749 experiences with ZebraNet. *SIGPLAN Not.* **37**, 96-107 (2002).
750 10. Toledo, S., Kishon, O., Orchan, Y., Shohat, A. & Nathan, R. in Software Science, Technology
751 and Engineering (SWSTE), 2016 IEEE International Conference on 51-60 (IEEE, 2016).
752 11. Rutz, C. et al. Automated mapping of social networks in wild birds. *Curr. Biol.* **22**, R669-R671
753 (2012).
754 12. Ayele, E.D., Meratnia, N. & Havinga, P.J. in New Technologies, Mobility and Security (NTMS),
755 2018 9th IFIP International Conference on 1-5 (IEEE, 2018).
756 13. Ripperger, S. et al. Automated proximity sensing in small vertebrates: design of miniaturized
757 sensor nodes and first field tests in bats. *Ecology and Evolution* **6**, 2179-2189 (2016).
758 14. Wilkinson, G.S. et al. Kinship, association, and social complexity in bats. *Behav. Ecol.*
759 *Sociobiol.* **73**, 7 (2019).
760 15. Sekara, V., Stopczynski, A. & Lehmann, S. Fundamental structures of dynamic social
761 networks. *Proceedings of the national academy of sciences* **113**, 9977-9982 (2016).
762 16. Kilian, G. et al. Increasing Transmission Reliability for Telemetry Systems Using Telegram
763 Splitting. *IEEE Transactions on Communications* **63**, 949-961 (2015).
764 17. Schadhauser, M., Robert, J. & Heuberger, A. in Smart SysTech 2017; European Conference
765 on Smart Objects, Systems and Technologies 1-8 (VDE, 2017).
766 18. Hallworth, M.T. & Marra, P.P. Miniaturized GPS tags identify non-breeding territories of a
767 small breeding migratory songbird. *Scientific reports* **5**, 11069 (2015).
768 19. Cvikel, N. et al. Bats Aggregate to Improve Prey Search but Might Be Impaired when Their
769 Density Becomes Too High. *Curr. Biol.* **25**, 206-211 (2015).
770 20. Conenna, I., López-Baucells, A., Rocha, R., Ripperger, S. & Cabeza, M. Movement
771 seasonality in a desert-dwelling bat revealed by miniature GPS loggers. *Movement ecology* **7**,
772 1-10 (2019).
773 21. Tomkiewicz, S.M., Fuller, M.R., Kie, J.G. & Bates, K.K. Global positioning system and
774 associated technologies in animal behaviour and ecological research. *Philosophical*
775 *Transactions of the Royal Society B: Biological Sciences* **365**, 2163-2176 (2010).
776 22. Dressler, F. et al. Monitoring Bats in the Wild: On Using Erasure Codes for Energy-Efficient
777 Wireless Sensor Networks. *ACM Transactions on Sensor Networks (TOSN)* **12**, 1-29 (2016).

778 23. Cassens, B. et al. in Proceedings of the 2019 International Conference on Embedded
779 Wireless Systems and Networks 59-70 (Junction Publishing, 2019).
780 24. St Clair, J. et al. Experimental resource pulses influence social-network dynamics and the
781 potential for information flow in tool-using crows. *Nature Communications* **6**, 7197 (2015).
782 25. O'Mara, M.T., Wikelski, M. & Dechmann, D.K. 50 years of bat tracking: device attachment and
783 future directions. *Methods in Ecology and Evolution* **5**, 311-319 (2014).
784 26. Duda, N. et al. in 2019 IEEE Topical Conference on Wireless Sensors and Sensor Networks
785 (WiSNet) 1-4 (IEEE, 2019).
786 27. Kays, R. et al. Tracking Animal Location and Activity with an Automated Radio Telemetry
787 System in a Tropical Rainforest. *The Computer Journal* (2011).
788 28. Nowak, T., Hartmann, M., Tröger, H.-M., Patino-Studencki, L. & Thielecke, J. in 2017 IEEE
789 International Conference on Communications Workshops (ICC Workshops) 1024-1029 (IEEE,
790 2017).
791 29. Kerth, G., Perony, N. & Schweitzer, F. Bats are able to maintain long-term social relationships
792 despite the high fission–fusion dynamics of their groups. *Proceedings of the Royal Society B:*
793 *Biological Sciences* **278**, 2761-2767 (2011).
794 30. Aplin, L.M. et al. Experimentally induced innovations lead to persistent culture via conformity
795 in wild birds. *Nature* **518**, 538-541 (2015).
796 31. Lopes, P.C., Block, P. & König, B. Infection-induced behavioural changes reduce connectivity
797 and the potential for disease spread in wild mice contact networks. *Scientific reports* **6**, 31790
798 (2016).
799 32. Levin, I.I. et al. Stress response, gut microbial diversity and sexual signals correlate with social
800 interactions. *Biol. Lett.* **12**, 20160352 (2016).
801 33. Saltzer, J.H., Reed, D.P. & Clark, D.D. End-to-end arguments in system design. *ACM*
802 *Transactions on Computer Systems* **100**, 277-288 (1984).
803 34. Schmidt, A. et al. Cross-Layer Pacing for Predictably Low Latency. *Proc. 6th Intl. Worksh. on*
804 *Ultra-Low Latency in Wireless Networks (Infocom ULLWN). IEEE* (2019).
805 35. Blobel, J. & Dressler, F. in 2017 IEEE Conference on Computer Communications Workshops
806 (INFOCOM WKSHPS) 984-985 (IEEE, 2017).
807 36. Nabeel, M., Amjad, M.S. & Dressler, F. in 2018 IEEE Global Communications Conference
808 (GLOBECOM) 1-6 (IEEE, 2018).

37. Teitelbaum, C.S. & Mueller, T. Beyond Migration: Causes and Consequences of Nomadic Animal Movements. *Trends Ecol. Evol.* (2019).

38. Stroeymeyt, N. et al. Social network plasticity decreases disease transmission in a eusocial insect. *Science* **362**, 941-945 (2018).

39. Consortium, T.Q. Networking Our Way to Better Ecosystem Service Provision. *Trends Ecol. Evol.* **31**, 105-115 (2016).

40. Nowak, T., Hartmann, M., Zech, T. & Thielecke, J. in 2016 IEEE-APS Topical Conference on Antennas and Propagation in Wireless Communications (APWC) 110-113 (IEEE, 2016).

41. Nowak, T., Hartmann, M. & Thielecke, J. Unified performance measures in network localization. *EURASIP Journal on Advances in Signal Processing* **2018**, 48 (2018).

42. Hartmann, M., Nowak, T., Pfandenhauer, O., Thielecke, J. & Heuberger, A. in 2016 12th Annual Conference on Wireless On-demand Network Systems and Services (WONS) 1-8 (IEEE, 2016).

43. Nowak, T., Hartmann, M. & Thielecke, J. in 2018 11th German Microwave Conference (GeMiC) 115-118 (IEEE, 2018).

44. Nowak, T., Hartmann, M., Patino-Studencki, L. & Thielecke, J. in 2016 13th Workshop on Positioning, Navigation and Communications (WPNC) 1-6 (IEEE, 2016).

45. Duda, N. et al. BATS: Adaptive Ultra Low Power Sensor Network for Animal Tracking. *Sensors* **18**, 3343 (2018).

46. Hijmans, R.J., Williams, E., Vennes, C. & Hijmans, M.R.J. in Spherical trigonometryv 1.5-7 (2019).

47. Schadhauser, M., Robert, J. & Heuberger, A. in Smart SysTech 2016; European Conference on Smart Objects, Systems and Technologies 1-9 (VDE, 2016).

48. Wägemann, P., Dietrich, C., Distler, T., Ulbrich, P. & Schröder-Preikschat, W. Whole-system worst-case energy-consumption analysis for energy-constrained real-time systems. *Leibniz International Proceedings in Informatics, LIPIcs 106 (2018)* **106**, 24 (2018).

49. Schirmer, A., Herde, A., Eccard, J.A. & Dammhahn, M. Individuals in space: personality-dependent space use, movement and microhabitat use facilitate individual spatial niche specialization. *Oecologia* **189**, 647-660 (2019).

50. Ripperger, S. et al. Proximity sensors on common noctule bats reveal evidence that mothers guide juveniles to roosts but not food. *Biol. Lett.* **15**, 20180884 (2019).

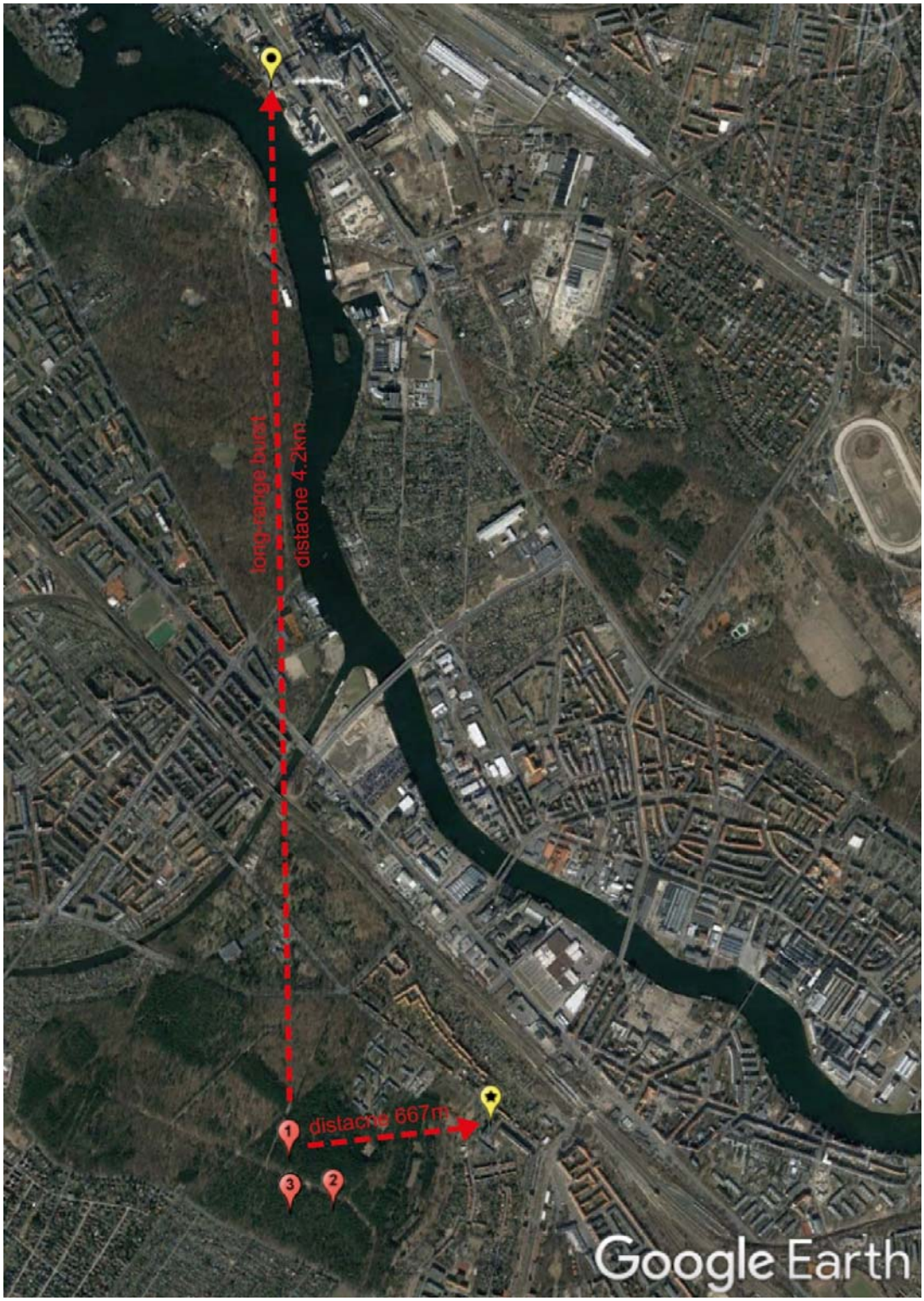

Supplementary Figure 1: Experimental setup for long-range telemetry in the city of Berlin, Germany. Yellow symbols mark the positions of two long-range telemetry receivers (asterix = retirement home, circle = cogeneration plant). Red symbols show the locations of bat day roosts 1 to 3 (tree holes). Map data ©2019 GeoBasis-DE/BKG (©2009), Google.

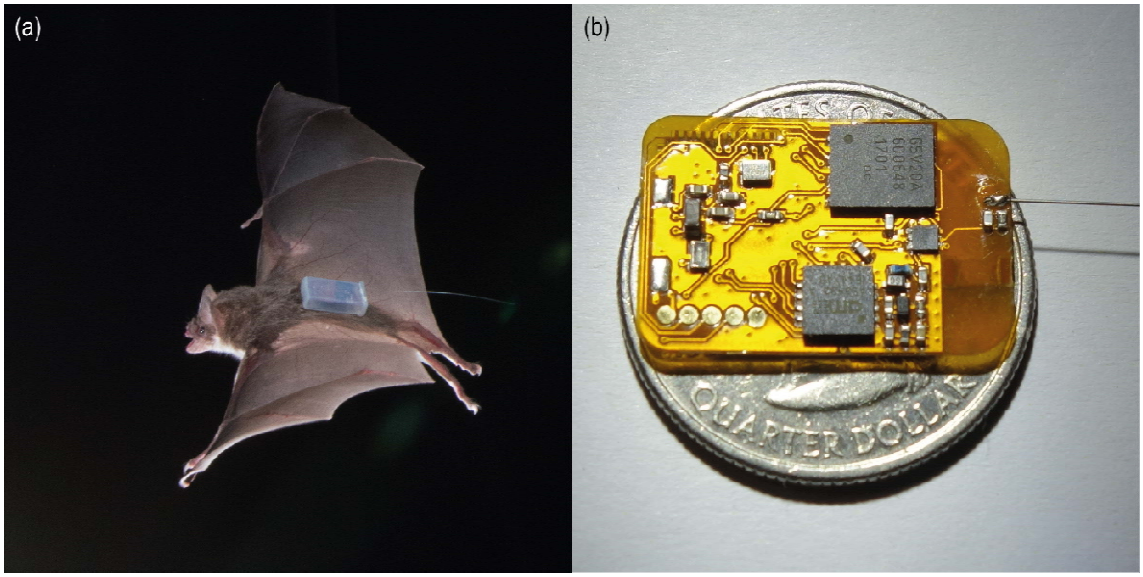

Supplementary Figure 2: animal-borne mobile node for proximity sensing. (a) Common vampire bat (*Desmodus rotundus*) carrying a mobile node housed in a plastic case; (b) bare mobile node on a quarter US dollar coin for comparison of size .

Supplementary Table 1: Glossary. Description of hardware components, communication and data types and software tasks considered for the energy model.

Keyword	**Description**
Hardware	
Mobile node (MN)	Animal-borne sensor node.
Ground node (GN)	Multifunctional ground-based sensor nodes. Depending on the GN-configuration, it receives data from MNs, triggers transmission of localization packets at the MN, or triggers the transmission of presence signals at the MN.
Localization node	Sensor node containing a dual-band antenna for high-resolution positioning of MNs. Arranged in a tracking grid.
Long-range receiver	Long-range telemetry-dedicated sensor node for receiving long-range bursts.

Communication and data types	
Ground node beacon (GN-beacon)	A packet sent by a ground node that triggers action on the MN (e.g., data download).
Mobile node beacon (MN-beacon)	A packet sent by a mobile node. It contains a wakeup sequence which wakes other MNs from standby.
Long-range burst	A packet embedded in the wakeup sequence of the MN-beacon for data transmission to a long-range receiver.
Localization packet	A packet sent by a MN to localization nodes for high-resolution tracking. Transmission is initiated by a GN-beacon.
Presence Signal	A packet sent by a MN to indicate the presence of a bat in range of a GN. Transmission is initiated by a GN-beacon.
Software task on the mobile node	
(i) standby	An idle state where only mandatory devices are active (e.g., wakeup receiver). The idle state is terminated by the reception of a wakeup.
(ii) sending beacons	Sending a MN-beacon to wake nearby MNs from standby. Nearby MNs immediately send their IDs in return.
(iii) receiving beacons	If the wakeup receiver receives a wakeup sequence, the conventional receiver is activated to receive the IDs of nearby MNs (encoded in the MN-beacons).
(iv) observing ground node availability	Every 2 s the receiver is activated to check whether GN-beacons are received.
(v) transmitting data to a ground node	If beacons of a download-dedicated GN are received, the transmitter is activated and data download is initiated.
(vi) sending localization packets	If beacons of a tracking-dedicated GN are received, localization packets are sent (duty cycle 8/s; 868MHz & 2.4GHz)
(vii) sending presence signals	If beacons of a GN are received, a presence signals is send